

Tungsten Targets the Tumor Microenvironment to Enhance Breast Cancer Metastasis

Alicia M. Bolt^{*,†}, Valérie Sabourin^{*}, Manuel Flores Molina^{*}, Alice M. Police^{‡,§}, Luis Fernando Negro Silva^{*,¶}, Dany Plourde^{*}, Maryse Lemaire^{*,†}, Josie Ursini-Siegel^{*,†,¶}, and Koren K. Mann^{*,†,¶,1}

^{*}Lady Davis Institute for Medical Research, McGill University, Montréal, Québec, Canada, H3T 1E2, [†]Department of Oncology, McGill University, Montréal, Québec, Canada, H2W 1S6, [‡]Pacific Breast Care Center, Costa Mesa, California, 92627, [§]Division of Surgical Oncology, University of California, Irvine School of Medicine, Irvine, California, 92627; and [¶]Division of Experimental Medicine, McGill University, Montréal, Québec, Canada, H3A 1A3

¹To whom correspondence should be addressed Lady Davis Institute for Medical Research, 3755 Côte Ste Catherine Road, Rm E537, Montréal, Québec, Canada H3T 1E2. Fax: 514-340-8717 E-mail: koren.mann@mcgill.ca.

ABSTRACT

The number of individuals exposed to high levels of tungsten is increasing, yet there is limited knowledge of the potential human health risks. Recently, a cohort of breast cancer patients was left with tungsten in their breasts following testing of a tungsten-based shield during intraoperative radiotherapy. While monitoring tungsten levels in the blood and urine of these patients, we utilized the 66Cl4 cell model, *in vitro* and in mice to study the effects of tungsten exposure on mammary tumor growth and metastasis. We still detect tungsten in the urine of patients' years after surgery (mean urinary tungsten concentration at least 20 months post-surgery = 1.76 ng/ml), even in those who have opted for mastectomy, indicating that tungsten does not remain in the breast. In addition, standard chelation therapy was ineffective at mobilizing tungsten. In the mouse model, tungsten slightly delayed primary tumor growth, but significantly enhanced lung metastasis. *In vitro*, tungsten did not enhance 66Cl4 proliferation or invasion, suggesting that tungsten was not directly acting on 66Cl4 primary tumor cells to enhance invasion. In contrast, tungsten changed the tumor microenvironment, enhancing parameters known to be important for cell invasion and metastasis including activated fibroblasts, matrix metalloproteinases, and myeloid-derived suppressor cells. We show, for the first time, that tungsten enhances metastasis in an animal model of breast cancer by targeting the microenvironment. Importantly, all these tumor microenvironmental changes are associated with a poor prognosis in humans.

Key words: tungsten; metastasis; tumor microenvironment; breast cancer

Tungsten is a naturally occurring transition metal that has many desirable characteristics including strength and flexibility. In the general population, individuals can be exposed to trace amounts of tungsten in food, drinking water, and air. Until recently, tungsten was thought to be an "inert" metal having low toxicity, which has led to its incorporation into a wide range of industrial goods and medical devices (Keith *et al.*, 2007). Increased use of tungsten has resulted in increased contamination of air, soil, and water, especially near active tungsten mines or industrial sites. Due to this increase in contamination, the

number of individuals exposed to high levels of tungsten is on the rise. A unique population at risk of tungsten exposure includes patients exposed to implanted medical devices containing tungsten. During a clinical trial in 2011, breast cancer patients were exposed to tungsten from a tungsten-based shield that was placed internally during intraoperative radiotherapy (clinicaltrials.gov: NCT01189851). The shield left residual tungsten particles in patient's breast tissue, which increased the tungsten exposure levels in these women. These recent exposures to high levels of tungsten have raised public awareness

and concern, regarding the lack of information of the potential toxic effects of tungsten exposure and long-term human health risks. In fact, the Environmental Protection Agency (EPA) classified tungsten as an emerging contaminant that warrants further toxicological investigation (EPA, 2008).

Currently, very little is known regarding the potential carcinogenic effects of tungsten. Although epidemiological data are lacking, *in vitro* and *in vivo* studies provide evidence that tungsten may contribute to cancer progression. Tungsten-containing alloys are genotoxic *in vitro* (Anard et al., 1997) and have the ability to transform an osteoblast cell line (Miller et al., 2001). When tungsten alloy-based bullets were implanted in rats to test the effects of embedded ammunition shrapnel in wounded soldiers, 100% of the rats developed rhabdomyosarcoma (Kalinich et al., 2005). One limitation of these studies is that the alloys used contained not only tungsten, but also other metals, such as nickel and cobalt, which are also known carcinogens (Beyersmann and Hartwig, 2008). The individual contribution of tungsten in these experiments is not known. However, tungsten alone increased the incidence of cancer in rats using a mutagen-induced cancer model, providing evidence that tungsten may act as a tumor promoter (Wei et al., 1985). In addition, we have determined that tungsten can induce DNA damage and increase the clonogenic ability of B cells in the bone marrow (Kelly et al., 2012).

We are currently monitoring this unique cohort of breast cancer patients accidentally exposed to tungsten. However, given the limited data investigating the role of tungsten on cancer progression and metastasis, it is impossible to predict the potential effects of tungsten exposure, particularly in regards to their risk of recurrence or metastases. Thus, in this study, we investigated the role of tungsten on breast cancer progression and metastasis using a preclinical mouse model and provide the first experimental evidence that tungsten exposure can significantly enhance the lung metastatic potential of breast cancer cells in mice by stimulating a protumorigenic inflammatory microenvironment in the metastatic niche.

MATERIALS AND METHODS

Patient Data

All patient samples were obtained with patient consent approved by the Jewish General Hospital Research Ethics Committee (Montréal, Quebec, Canada). Breast biopsy samples were fixed and paraffin embedded. Serial sections were stained with hematoxylin and eosin (H&E). Tungsten concentration in blood and urine samples was assessed by inductively coupled plasma mass spectroscopy (ICP-MS) analyses by Doctor's Data (St. Charles, Illinois). Patients received chelation therapy of either dimercaptopropanesulfonic acid (DMPS) or dimercaptosuccinic acid (DMSA). Urine samples were collected pre- and post-treatment for each patient and analyzed for tungsten concentration.

Orthotopic Breast Cancer Model

Tumor cell line. 66Cl4 cells are a resistant variant of the tumor cell subpopulation line 66, which is part of the Miller panel of mammary tumor cell lines, all isolated from a single spontaneously arising tumor from a BALB/c mouse (Dexter et al., 1978). Cells were cultured in RPMI media (Wisent, St. Bruno, Quebec, Canada) supplemented with 10% fetal bovine serum (FBS; Wisent) and 1% penicillin/streptomycin (Wisent) at 5% CO₂ and 37°C.

Mice. Female BALB/c mice (6–8 weeks old) were purchased from Charles Rivers Laboratories Inc (Montréal, Quebec, Canada) and

housed in the Lady Davis Institute Animal Care Facility. Animal experiments were approved by the McGill University Animal Care Committee (Montréal, Quebec, Canada). Mice were given food and water *ad libitum*. Mice were divided into 2 groups: control tap water or 15 parts per million (ppm; µg/ml) sodium tungstate dihydrate (Na₂WO₄·2H₂O; Sigma-Aldrich, St. Louis, Missouri) was dissolved in tap water and replaced every 2 or 3 days to limit conversion to polytungstates (Kelly et al., 2012). After 1 week of acclimatization, mice were exposed to tap water or tungsten in drinking water for 4 weeks prior to tumor cell injection and remained exposed for the duration of the study. As we have previously published in C57BL/6J mice (Kelly et al., 2012), no changes in animal weight, physical appearance, or water intake were observed in the tungsten-exposed group. After the 4-week exposure, 66Cl4 cells (50 000) were injected into the fourth mammary fat pad of control and tungsten-exposed mice. Tumor size was determined using calipers every 3–4 days. Tumor volume was calculated using the following equation, volume = (4/3 × (3.14159) × (length/2) × (width/2)²) and the maximum tumor volume was 1000 mm³. Once tumor-size endpoint was reached (25–36 days), mice were euthanized with terminal cardiac puncture. Primary tumors were excised, sections were fixed in 10% buffered formalin (Thermo Fisher Scientific, Waltham, Massachusetts) and paraffin-embedded (Jewish General Hospital Pathology Department, Montréal, Quebec, Canada). A set of non-tumor-bearing BALB/c mice was also used as treatment controls for the experiment. Non-tumor-bearing mice were given tap water or water containing 15 ppm sodium tungstate dihydrate for 8 weeks.

Plasma Analyses

Total blood cell counts were performed using a Scil Vet abc Hematology Analyzer (Scil Vet Novations, Barrie, Ontario, Canada). Blood was collected in EDTA-containing tubes (Thermo Fisher Scientific) prior to tumor cell injection and then weekly throughout tumor growth via saphenous vein puncture. At the end of the experiment, blood was collected in EDTA-containing tubes (0.6 ml, BD Biosciences, Mississauga, Ontario, Canada) by cardiac puncture and cells were counted. Remaining peripheral blood was centrifuged, cells were collected for white blood cell characterization, and plasma was collected for tungsten quantification and matrix metalloproteinase zymography.

Metastasis Analyses in Lung

Lung lobes were dissected, fixed in 10% buffered formalin and paraffin embedded as previously described for the tumor samples. The number of metastases per lobe was analyzed in 5 step-wise sections (50 µm apart) per animal, which had been stained with H&E. Average metastasis size was determined by measuring the area of each lesion at the largest point of the 5 sections using Image J software (NIH, Bethesda, Maryland). Percent tumor burden was calculated per lobe and averaged per animal.

Immunohistochemistry

Staining was performed on sections of paraffin-embedded tumor and lung tissue. Antigen retrieval was performed in sodium citrate buffer. Primary antibodies were incubated at 4°C overnight at the following dilutions: Ki67 (1:1000, Abcam, Toronto, Ontario, Canada), cleaved caspase-3 (1:300, Cell Signaling, Danvers, Massachusetts), Gr1 (1:200, R&D Systems, Minneapolis, Minnesota), and α-smooth muscle actin (α-SMA) (1:250, Sigma-Aldrich). Biotinylated-secondary antibodies were

incubated at room temperature for 30 min and then slides were processed using the peroxidase VECTASTAIN ABC kit (Vector Laboratories, Burlingame, California). Slides were developed with ImmPACT DAB peroxidase substrate (Vector Laboratories). Sections were counterstained with 20% Harris modified hematoxylin (Thermo Fisher Scientific). Sections were mounted in Permount (Thermo Fisher Scientific). Slides were scanned using an Aperio Scanscope AT Turbo scanner (Leica Biosystems, Concord, Ontario, Canada). The number of Ki67 positive nuclei in primary tumor and metastatic lesions was assessed by manual nuclei counts of tissue images using ImageJ (NIH). For metastatic lesion analysis, 10 representative regions of metastatic lesion tissue from control and tungsten-exposed lung sections were counted. For primary tumor sections, 5 independent regions per tumor section were counted and averaged per section. Ki67 data were represented as the percent positive cells versus total number of cells (positive and negative) per counted section. Cleaved caspase-3, α -SMA, and Gr1 stained sections were analyzed using Aperio ScanScope software (Leica Biosystems). The percentage of cleaved caspase-3 in tumor sections was calculated by measuring the area of each tumor section positive for cleaved caspase-3 in comparison to total area of tumor section. Gr1 and α -SMA staining was analyzed within and directly surrounding metastatic lesions using the positive pixel count analysis algorithm. For the α -SMA analysis, total positive pixels was determined by the sum of strong and medium intensity pixels. For the Gr1 analysis, the total number of strong and medium pixels was less per lesion so total positive pixels also included the number of weak intensity pixels. A total of 45 lesions (Gr1 staining) and 70 lesions (α -SMA staining) containing positive staining was analyzed. One large outlying lesion was excluded from the tungsten-exposed group in the α -SMA staining analysis. To correct for this, the largest control lesion was also excluded from the analysis. Data are represented as the mean number of positive pixels per lesion. α -SMA data were additionally analyzed by stratifying data into 3 equal groups (large, medium, and small lesions) based on lesion area. Positive α -SMA staining in normal lung tissue was analyzed as described previously. Normal lung staining data were normalized to total area of each lobe.

Tungsten Analyses

Bone marrow was flushed from tibiae bones and empty bones were stored at -20°C . Elemental tungsten concentration in bone and plasma was assessed by ICP-MS analyses by Chemical Solutions Ltd (Mechanicsburg, Pennsylvania) with a detection limit of 0.1 ppm for bone and 0.1 parts per billion (ppb; ng/ml) for plasma samples.

Matrix Metalloproteinase Zymography

Plasma from tumor-bearing mice or equal volumes of 66Cl4 conditioned media was subjected to SDS-PAGE on 7.5% acrylamide gel copolymerized with 0.1% gelatin. Conditioned media was obtained from 66Cl4 cells (50000 cells; control and tungsten-exposed for 4 weeks) that were cultured in serum-free media for 96 h and concentrated using Amicon Ultra-4 Centrifugal Filter Concentrators (EMD Millipore, Division of Merck, Darmstadt, Germany). Gels were washed in 2.5% Triton X-100 solution, incubated for 24 h at 37°C in reaction solution (50 mM Tris, 5 mM CaCl_2 , and 200 mM NaCl), and fixed in 50% methanol and 10% acetic acid. Bands were visualized by staining with Coomassie and imaged using the Chemi Genius² Bio Imaging System (Syngene, Frederick, Maryland). Band densitometry was calculated using ImageJ (NIH).

White Blood Cell Characterization

Peripheral blood was centrifuged and plasma was removed. Red blood cells were lysed with Tris-buffered ammonium chloride lysis buffer. Remaining white blood cells were stained with Live/Dead Fixable Aqua 405 nm (Molecular Probes, Burlington, Ontario, Canada). Samples were blocked in Fc block CD16/CD32 (BD Biosciences) and stained with primary fluorescently conjugated antibodies Gr1-AF488 (eBioscience, San Diego, California) and CD11b-APC (eBioscience) for 30 min at 4°C . Samples were analyzed by flow cytometry using an LSR Fortessa Cell Analyzer (BD Biosciences). Data were analyzed using FlowJo software (Ashland, Oregon).

66Cl4 Cell Proliferation

66Cl4 cells were cultured in 10 cm dishes, under the same culture conditions mentioned above. 66Cl4 (1×10^6) were exposed to a range of low-dose sodium tungstate dihydrate concentrations (0, 0.25, 0.5, 1, 2, and 4 ppb). Cells were passaged every 2 days to maintain the cells in an exponential growth phase. Cell density was monitored for 10 days by counting cells using the trypan blue exclusion assay at each passage. Cell growth for each exposure group was calculated by multiplying the total number of viable cells (trypan blue negative) by the dilution factors from previous passages.

Invasion Assay

66Cl4 cells (control and sodium tungsten dihydrate-exposed for 4 weeks) were serum starved overnight before starting assay. As a positive control, 66Cl4 cells were exposed to 5 ng/ml TGF β for 96 h (serum starved for the last 16 h). Cells (75 000/ml) in serum-free media containing 0.1% bovine serum albumin (Sigma-Aldrich) were cultured on the upper membrane (pores: 8.0 μm) of Bowden chamber (Corning, Tewksbury, Massachusetts) coated with 6 μg of Matrigel (BD Biosciences). After a 20-h incubation, cell migration toward the chemoattractant (10% FBS in RPMI) in the lower chamber was assessed. Membranes were fixed in 5% glutaraldehyde (Sigma-Aldrich) and stained with 0.005% crystal violet (Sigma-Aldrich). Migrated cells were imaged using an Infinity 3 camera mounted on a Leica light microscope and counted using ImageJ (NIH).

Statistics

All statistics were performed using GraphPad Prism version 4 software (GraphPad, La Jolla, California). For comparisons between 2 groups, an unpaired Student's *t* test analysis was performed. For comparisons between 3 or more groups, either a 1-way or 2-way ANOVA analysis was performed based on the number of continuous variables analyzed. For correlation analyses, a Spearman correlation analysis was performed.

RESULTS

Patients Have Measurable Tungsten Levels That Are Not Mobilized by Standard Chelators

During a recent clinical trial, a tungsten-based, flexible shield was assessed in women undergoing intraoperative radiotherapy for breast cancer. During lumpectomy, the tungsten-based shield was inserted under the breast tissue to protect internal organs from radiation. Following the procedure, patients received follow-up standard digital mammography to evaluate treatment effectiveness. Mammography showed calcium-like densities in the breast tissue (Fig. 1A). Subsequent biopsies confirmed that those deposits were tungsten particles that had remained in the breast tissue following the operation. Tungsten

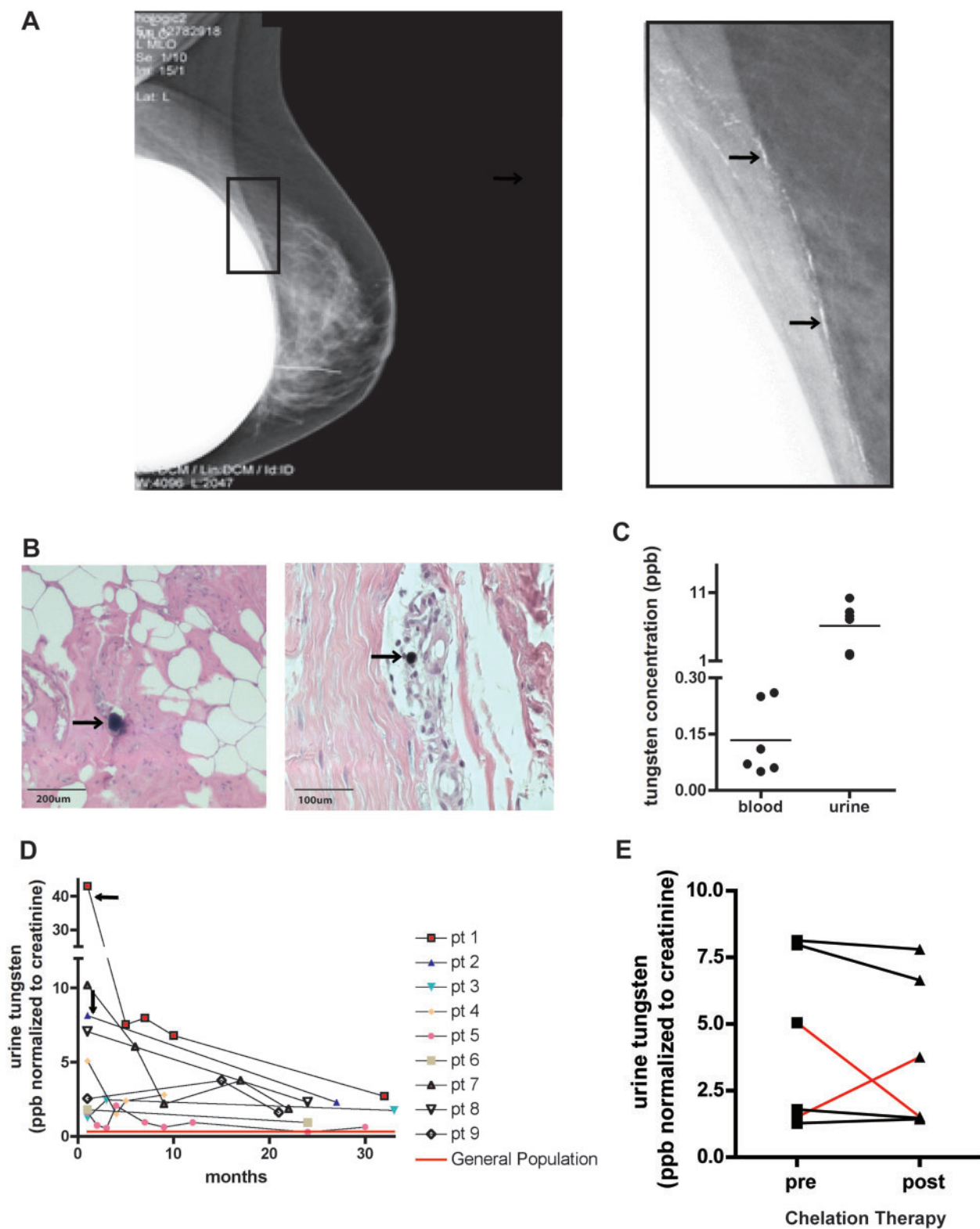


FIG. 1. Breast cancer patients were exposed to tungsten during a recent clinical trial. **A**, Digital mammography image of a patient's breast post-surgery. Enlarged image shows white deposits (black arrows) that were biopsy-confirmed to be tungsten particles. **B**, Representative images of H&E-stained breast tissue from a patient who opted for a mastectomy (Left, 10 \times , Right, 20 \times). Black arrows indicate tungsten particles surrounded by inflammatory cells (purple cellular staining). **C**, Matched patient blood and urine tungsten concentrations (ppb). Graph shows samples where blood and urine samples were taken within a close timeframe and were collected between 0 and 5 months post-surgery. Graph represents the mean concentrations (horizontal line) among individual data points. **D**, Longitudinal monitoring of patient's urinary tungsten concentrations starting as soon as possible after point of exposure. In patients 1 and 2, black arrows indicate point of mastectomy to remove residual tungsten in the breast. Red line indicates average urinary tungsten levels for the general population in United States and Canada. **E**, Urinary tungsten concentrations pre- and post-chelation treatment. Lines indicate pre- and post-measurements for the same patient. Red lines indicate 1 patient that responded after first treatment (concentration increased), but then did not respond after second treatment (concentration decreased).

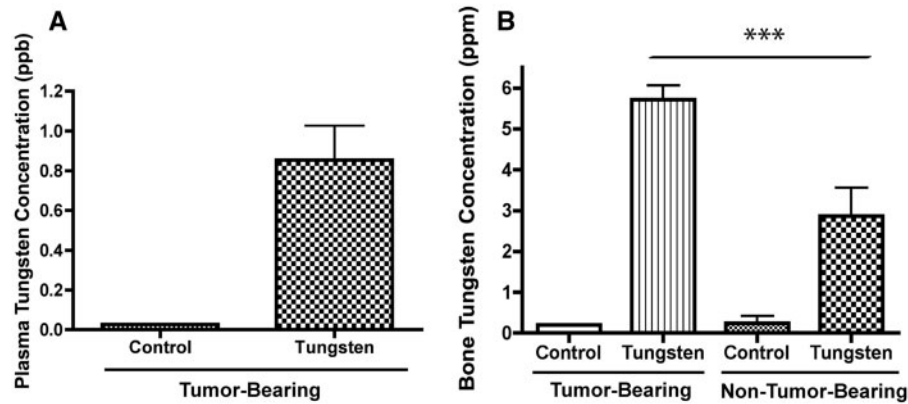


FIG. 2. Tungsten concentrations in the plasma and bone in the 66Cl4 orthotopic model. A, Plasma tungsten concentrations in control and tungsten-exposed, tumor-bearing mice. Graph shows mean \pm SE ($n=3$). B, Bone tungsten concentrations in control and tungsten-exposed, tumor-bearing and non-tumor-bearing mice. Graph shows mean \pm SE ($n=6$). *** $P < 0.001$, 1-way ANOVA.

particles could be found in the breast, often surrounded by inflammatory cells (Fig. 1B). In addition, tungsten was detectable in both the blood and urine of these patients, indicating that tungsten was not confined to the breast tissue, but rather had been mobilized into the circulation (Fig. 1C). Comparing matched blood and urine measurements shows that urine has 50 times more tungsten than the blood (blood mean = 0.13 ppb, urine mean = 6.13 ppb). Long-term monitoring of patient urine showed that tungsten was still detectable in all patients, even 2.5 years after surgery (Fig. 1D). The mean detectable urinary tungsten concentration found after at least 20 months post-surgery was 1.76 ppb. Furthermore, 2 patients opted for mastectomy to remove all residual tungsten from the breast tissue (Fig. 1D, black arrows), and tungsten urine levels were still elevated 2 years post-mastectomy (2.71 and 2.29 ppb, respectively). Importantly, these levels are 4 times higher than average reported urinary tungsten concentrations that range from 0.08 to 0.7 ppb in the general public (CDC, 2003; Health Canada, 2013; Paschal et al., 1998; Tyrrell et al., 2013). Patients received a standard chelation therapy of either DMPS or DMSA in an attempt to remove residual tungsten. This therapy effectively mobilizes other heavy metals deposited in the body including lead and copper (Planas-Bohne, 1979; Xu and Jones, 1988). However, the standard chelation therapy was not effective in mobilizing tungsten in these patients (Fig. 1E). One patient (red lines) initially had increased tungsten in the urine post-chelation, but a second round proved ineffective. Together these data indicate that in humans, a secondary tungsten reservoir can be created, which may provide a source of chronic exposure that is resistant to standard chelation therapy.

Tungsten Enhances Breast Cancer Metastasis in the Lung

To more effectively evaluate the potential risk of tungsten exposure on breast cancer tumor growth and the risk of metastasis, we utilized the breast cancer cell line 66Cl4, which when injected into the mammary fat pads of immunocompetent BALB/c mice, aggressively metastasizes to the lung. Clonogenic cells can be detected in the lung as early as Day 14, and all mice have detectable tumor cells in the lung by Day 28 post-injection (Aslakson and Miller, 1992). Mice were pre-exposed to tungsten orally for 1 month before tumor cell injection and remained on tungsten for the duration of the study. An oral concentration of 15 ppm of sodium tungstate was selected, because it is the lowest concentration at which we have observed tungsten-induced changes in

mice (Kelly et al., 2012). After the 2-month exposure, the mean plasma tungsten concentration in the tumor-bearing mice was 0.85 ppb (Fig. 2A), a plasma concentration that is slightly higher than plasma concentrations observed in the exposed women (Fig. 1C), but 1000 times lower than plasma concentrations observed in occupational exposures (NIOSH, 1977). We and others have shown that tungsten accumulates in the bone and can be a source of chronic exposure (Guandalini et al., 2011; Kelly et al., 2012). As expected, tungsten accumulates more in the bone (5.72 ppm) than in the plasma (0.85 ppb; Figs. 2A and 2B). Interestingly, the tumor-bearing mice had 2-times more tungsten present in the bone than their non-tumor-bearing counterparts, exposed to equivalent oral concentrations of tungsten. These data suggest that the presence of the primary mammary tumor is altering bone composition, which is in turn affecting tungsten deposition in the bone.

Primary tumor growth was monitored throughout the study in control and tungsten-exposed mice. Surprisingly, tungsten did not enhance primary tumor size; instead primary tumor growth was delayed in the tungsten-exposed mice (Fig. 3A). We evaluated cell proliferation and cell death in the primary tumors by immunohistochemistry (IHC). There was no change in the percentage of Ki67-positive nuclei in the tungsten-exposed, primary tumors (Fig. 3B). In addition, there was also no change in the percent of apoptotic cell death in the primary tumors, as analyzed by cleaved caspase-3 (Fig. 3C). This correlated with the data from 66Cl4 cells exposed to tungsten *in vitro*. 66Cl4 cells were grown for 10 days in a range of tungsten concentrations (0.25–4 ppb) similar to those observed in the plasma of exposed mice. We found that tungsten did not change the rate of 66Cl4 cell growth *in vitro* (Fig. 4A).

Next, we evaluated the extent of metastasis in the lung by analyzing step-wise H&E stained sections of tissue. Tungsten did not change the number of metastases per lobe in the lung, but the average size of each metastasis was 3-times larger in the tungsten-exposed mice (Fig. 3D). This resulted in a greater than 2-fold increase in the percent tumor burden per lobe of the lung. We evaluated cell proliferation in metastatic lesions by calculating the percentage of Ki67-positive nuclei by IHC. Tungsten-enhanced metastasis was associated with a 15% increase in the number of Ki67-positive cells in the metastatic lesions from tungsten-exposed mice (Fig. 3E). Thus, in contrast to the slight delay in primary tumor growth, tungsten exposure resulted in significantly larger breast cancer lung metastases

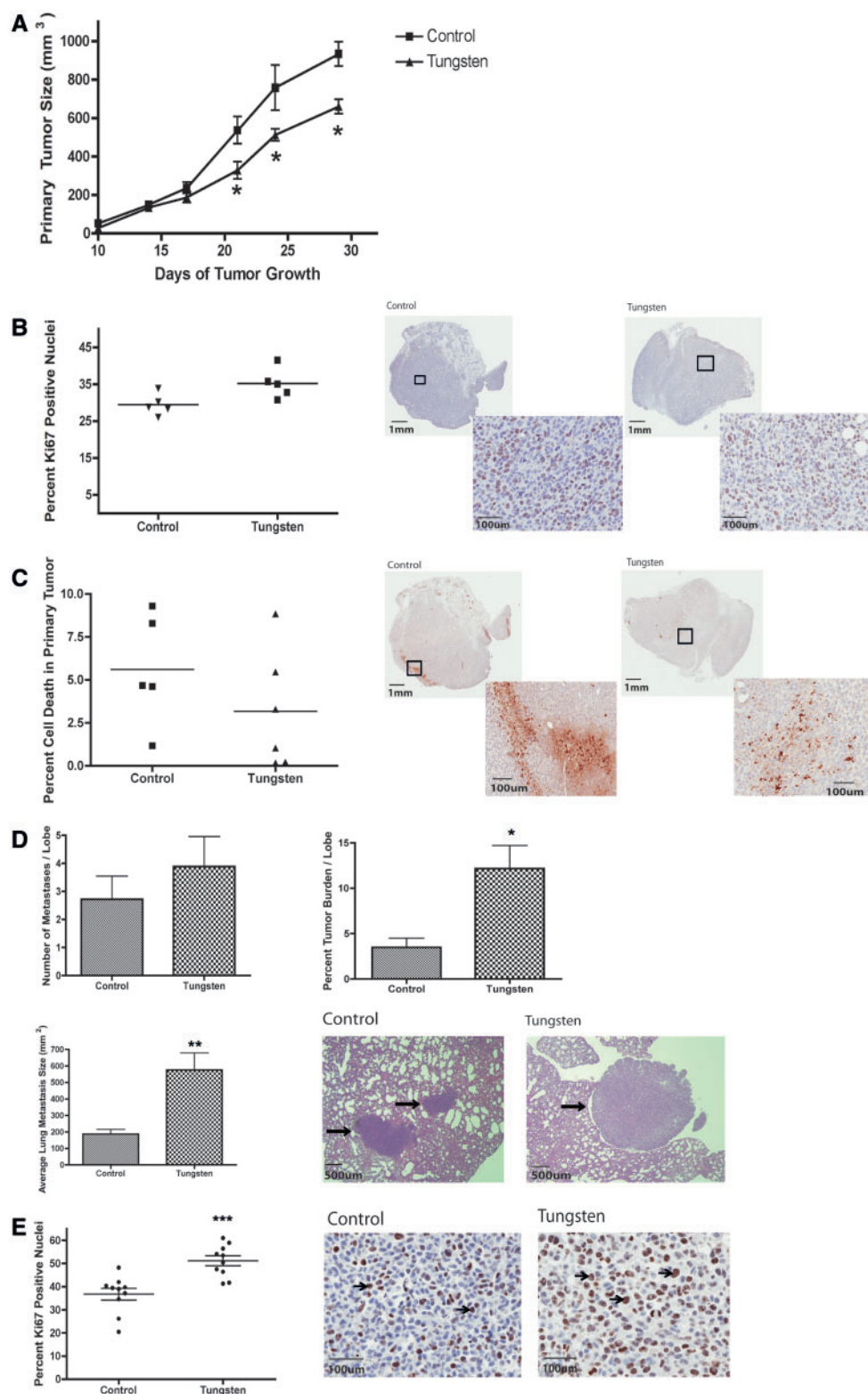


FIG. 3. Tungsten slightly delays primary mammary tumor growth, but significantly increases lung metastases. **A**, Primary tumor size was monitored throughout tumor progression. Graph represents the mean \pm SE for control and tungsten-exposed mice (control $n = 6$, tungsten $n = 7$). * $P < 0.05$, 2-way ANOVA. **B**, Percent Ki67-positive nuclei in primary tumor sections. Graph shows the mean (horizontal line) percent Ki67-positive nuclei per section for each group. Representative images of Ki67 stained tumor sections ($0.7\times$ and $20\times$). **C**, Percent cleaved caspase-3 in primary tumor sections. Graph shows the mean (horizontal line) percent area positive for cleaved caspase-3 per section per group. Representative images of cleaved caspase-3 stained tumor sections ($0.7\times$ and $20\times$). **D**, Lung metastasis analysis in tumor-bearing mice. Graphs show the mean \pm SE for the number of metastasis per lobe, the average size of metastasis per animal, and the percent tumor burden per lobe for each group (control: $n = 5$, tungsten: $n = 6$). * $P < 0.05$, ** $P < 0.01$ unpaired Student's t test. Representative images of H&E stained lung sections showing normal and metastatic (black arrows) tissue ($5\times$). **E**, Percent Ki67-positive nuclei in metastatic lesions. Graph represents the mean (horizontal line) \pm SE percent Ki67-positive nuclei per metastatic region for each group. *** $P < 0.001$ unpaired Student's t test. Representative images of Ki67 stained metastatic lesions ($20\times$). Arrows indicate Ki67-positive cells.

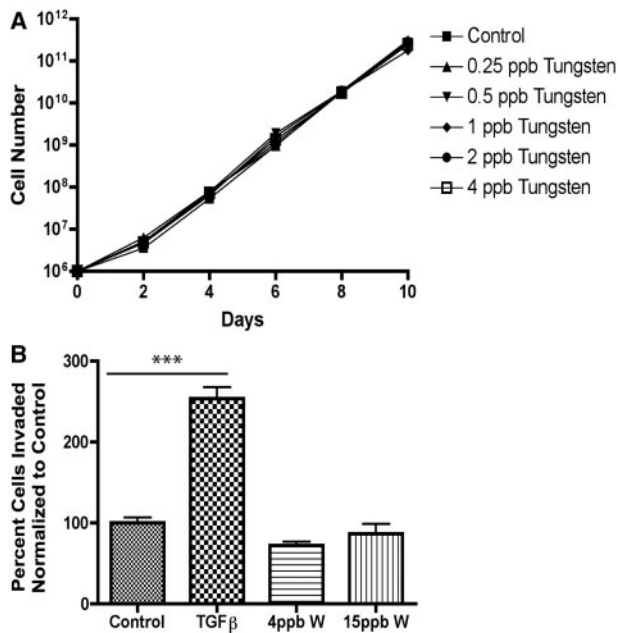


FIG. 4. Tungsten does not increase 66Cl4 proliferation or invasion *in vitro*. A, 66Cl4 growth was monitored over 10 days while cultured in a range of low-dose tungsten concentrations (0.25–4 ppb). Graph shows cell number (log 10) versus day for each concentration evaluated. B, 66Cl4 invasion assay through a matrigel matrix. 66Cl4 were cultured under control conditions or exposed to 4 or 15 ppb tungsten (W) for 4 weeks. Treatment with 5 ng/ml TGFβ for 96 h was used as a positive control. Graph shows the mean number of cells invaded \pm SE for each group, after normalization to control. For control and tungsten-exposed groups, data represent 5 replicate wells from 2 independent experiments. For TGFβ group, data represent 3 replicate wells.

owing to the specific ability of tungsten to augment tumor cell proliferation in the lung microenvironment.

Tungsten Does Not Change Invasiveness of Tumor Cells *in vitro*

We evaluated whether tungsten could directly increase the invasive potential of 66Cl4 cells through a matrigel matrix *in vitro*. Although treatment with 5 ng/ml TGFβ significantly increased 66Cl4 invasion, treatment with 4 or 15 ppb tungsten for 4 weeks did not (Fig. 4B). This is consistent with the observation that tungsten increased the size, but not the number of lung metastases, suggesting that it may indirectly affect the tumor cell by changing the tumor microenvironment at the metastatic site.

Tungsten Activates Cancer-Associated Fibroblasts at the Metastatic Site

Given that tungsten did not enhance the invasive potential of 66Cl4 cells *in vitro*, we hypothesized that tungsten exposure resulted in changes within the microenvironment that would promote metastases. Cancer-associated fibroblasts (CAFs) colonize the metastatic site where they play an active role in establishing metastatic foci and promoting metastatic growth and progression (Olaso *et al.*, 1997). CAFs have an active phenotype characterized by their expression of α -SMA (Yu *et al.*, 2014). Thus, we evaluated the metastatic lesions in the lung for evidence of activated fibroblasts that could promote metastasis by staining lung sections for α -SMA by IHC. Tungsten exposure was associated with an increase in α -SMA staining within the metastases (Fig. 5A). Interestingly, the amount of α -SMA staining was positively correlated with the size of the metastatic lesion regardless of exposure group (Spearman correlation

$r = 0.6728$, $P < 0.0001$). We stratified the analysis by size of metastatic lesion, and then compared α -SMA staining among large, medium, and small lesions. We found more α -SMA staining in medium and large, but not small lesions in the tungsten-exposed animals, although it was only statistically significant in the medium-sized lesions (Fig. 5B). We also determined whether tungsten increased activated fibroblasts in lung sections from non-tumor-bearing mice. Staining for α -SMA was primarily localized around the blood vessels in the lung and did not differ between control and tungsten-exposed mice (Fig. 5C).

CAFs secrete MMPs that degrade the extra cellular matrix (ECM) and thus, promote tumor progression and metastasis (Stuelten *et al.*, 2005). In particular, MMP-9 correlates with increased metastases in orthotopic breast cancer animal models (Nozaki *et al.*, 2003). We found that the tungsten-exposed mice had higher circulating levels of Pro-MMP-9 in the plasma than control animals (Figs. 6A and 6B). The expression of Pro-MMP-9 in the plasma was positively correlated with the average metastasis size per animal (Fig. 6C). Tungsten did not increase Pro- or active MMP-9 protein levels in conditioned media from 66Cl4 cells exposed *in vitro* (Fig. 6D) or in primary mammary tumors (Figs. 6E and 6F), further supporting our hypothesis that cells in the lung microenvironment are targets for tungsten.

Tungsten Increases the Number of Myeloid-Derived Suppressor Cells

In addition to CAFs, bone marrow-derived immune cells are critical regulators of metastasis that travel to secondary sites and prime the premetastatic niche to promote tumor cell migration and seeding (Kaplan *et al.*, 2005). In addition, we and others have shown that tungsten exposure alters the immune system (Fastje *et al.*, 2012; Kelly *et al.*, 2012). Therefore, we monitored changes in the peripheral blood by automated blood count to determine whether tungsten altered the peripheral immune response to the tumor. Although we found minor increases in the lymphocytic populations, we found that tungsten significantly enhanced the tumor-associated increase in granulocytic-like cells (Fig. 7A). This increase was most profound between Days 20 and 30 after tumor implantation (Fig. 7B). We did not observe any changes in the white blood cell profile in non-tumor-bearing mice in response to tungsten (Fig. 7C).

Within this granulocytic-like population, myeloid-derived suppressor cells (MDSCs) play a predominant role in tumor progression and metastasis. MDSCs are characterized by coexpression of 2 myeloid surface markers Gr1 (Ly6G) and CD11b (Kusmartsev *et al.*, 2004). Based on flow cytometric analysis of peripheral blood from tumor-bearing mice, the granulocytic-like cells present in the peripheral blood express both Gr1 and CD11b, suggesting that these are granulocytic-MDSC (Fig. 7D). We also assessed the MDSCs in the lung metastases of control and tungsten-exposed mice using Gr1 staining by IHC. Although not statistically significant, there was an increasing trend in Gr1 staining within the metastases of tungsten-exposed mice, supporting the hypothesis that tungsten may promote the infiltration of Gr1⁺/CD11b⁺ MDSCs that promote metastasis (Fig. 7E).

DISCUSSION

Given that the women presented in this study have residual tungsten in their bodies and there are currently no effective ways to remove the tungsten, it is vital to identify the potential risks of this exposure and try to remediate those toxicities. We specifically wanted to determine whether tungsten might alter the risk of breast cancer metastasis, as these women already

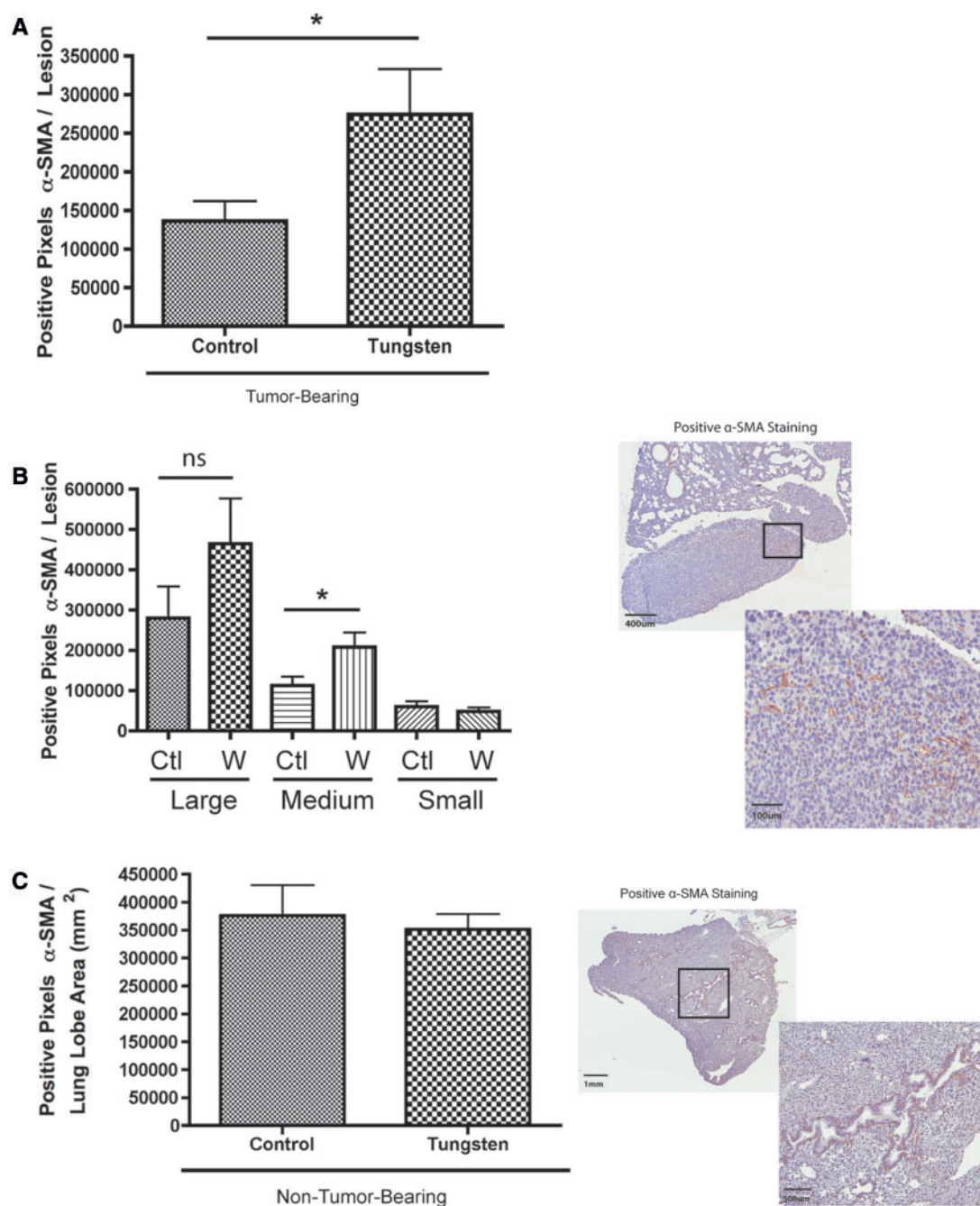


FIG. 5. Tungsten increases the α -SMA positive, cancer-associated fibroblasts at the metastatic site. A, Number of α -SMA positive pixels per metastatic lesion in the lung. Graph shows mean \pm SE for control and tungsten-exposed, metastatic lesions. * $P < 0.05$ unpaired Student's *t* test. B, Number of α -SMA positive pixels per metastatic lesion stratified by lesion size (C = control, W = tungsten). * $P < 0.05$ unpaired Student's *t* test per stratified pair. Representative images show positive α -SMA staining in metastatic lesions (6 \times and 20 \times). C, Number of α -SMA positive pixels per lobe in non-tumor-bearing mice lung tissue. Graph shows mean \pm SE for control and tungsten-exposed, non-tumor-bearing animals ($n = 8$ lung lobes). Representative images show positive α -SMA staining in normal lung tissue (2 \times and 4 \times).

have had primary tumors removed. In order to address this question, we evaluated the effect of tungsten on breast cancer tumor progression and metastasis both *in vitro* and using an orthotopic mouse model.

We show, for the first time, that tungsten exposure is linked with an increase in metastases in a mouse model of breast cancer. Although we did not identify direct effects on the tumor cells, tungsten exposure was associated with an increase in CAFs and MDSCs at the metastatic site. Furthermore, increased circulating levels of MMPs correlated with increased

metastatic lesions. Together, these data suggest that tungsten alters the tumor microenvironment to promote the growth of lung metastases. Importantly, we believe this is the first reported metal to target the tumor microenvironment instead of directly altering the primary tumor in order to promote tumor cell metastasis.

We found that the average size of metastases in the lung was significantly larger in the tungsten-exposed animals, which resulted in a greater percent tumor-burden per lobe, but we did not observe an increase in the number of metastases. However,

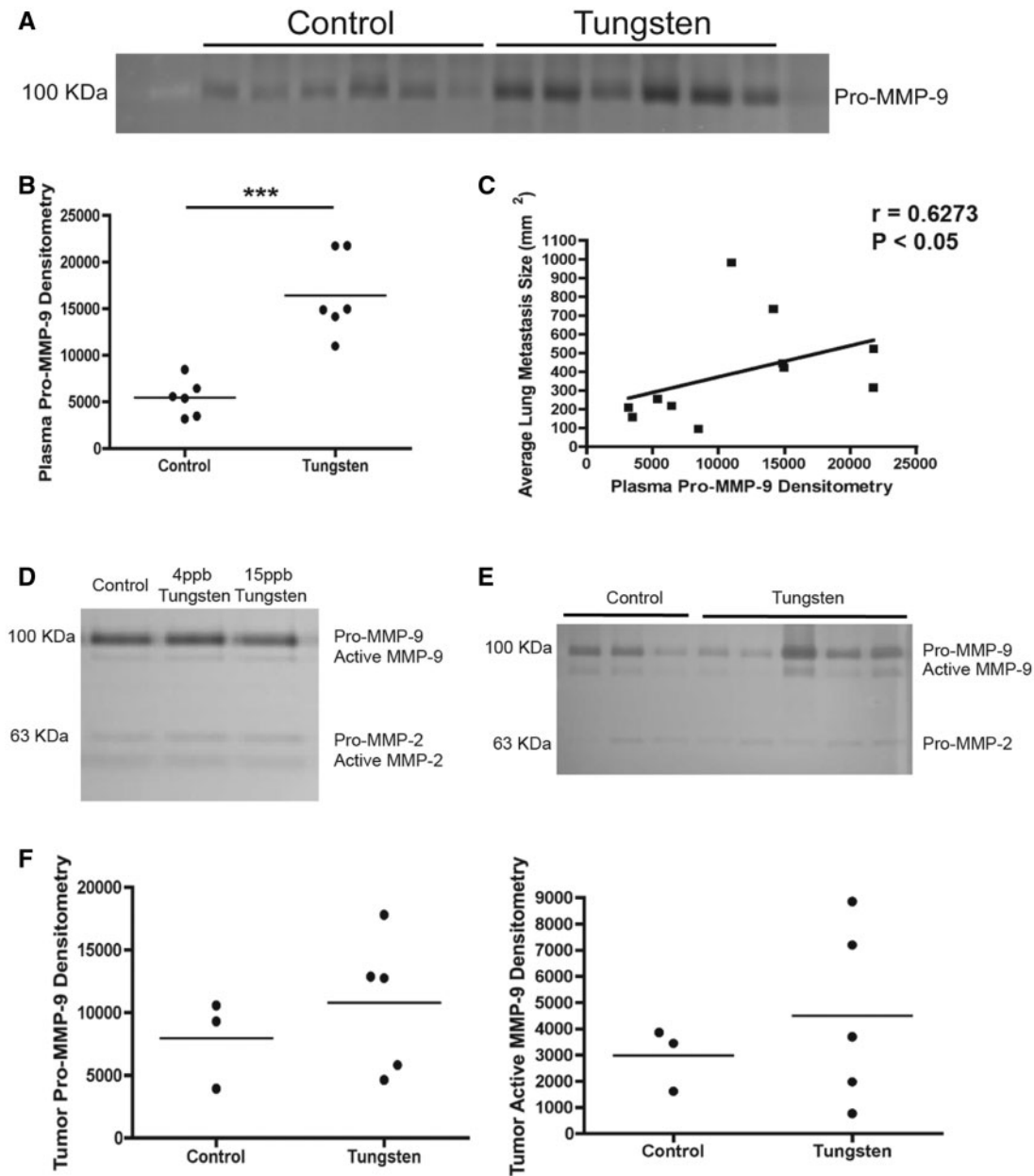


FIG. 6. Tungsten increases plasma levels of Pro-MMP-9. **A**, Image of zymography gel for Pro-MMP-9 in plasma samples from tumor-bearing (control and tungsten-exposed) animals. **B**, Band densitometry of zymography gel shown in **A**. Graph shows mean Pro-MMP-9 densitometry per group. *** $P < 0.001$ unpaired Student's *t* test. **C**, Spearman correlation analysis of plasma Pro-MMP-9 densitometry versus average metastatic lesion area per animal. **D**, Image of zymography gel for MMP-9 and MMP-2 in conditioned media from cultured 66Cl4 cells exposed to control, 4 or 15 ppb (4-week exposure) tungsten *in vitro*. Both the Pro- and Active forms of MMP-9 and MMP-2 were detected. **E**, Image of zymography gel for MMP-9 and MMP-2 in primary tumors. Both the Pro- and Active forms of MMP-9 and Pro-MMP-2 were detected. **F**, Band densitometry of zymography gel shown in **E**. Graphs show mean Pro-MMP-9 and Active MMP-9 densitometry per group.

lung metastases were only assessed at the end of the experiment, late in metastatic development. In order to fully determine the effects of tungsten exposure on the seeding and establishment of metastatic lesions, imaging the full progression of metastatic disease development is required. Also, we assessed metastases at only one site. Breast tumors commonly metastasize not only to the lung, but also the liver, bone, and brain (Chambers *et al.*, 2002). It will be important to test tungsten in other mouse models that can metastasize to these locations.

Of particular importance is the bone, because tungsten preferentially and rapidly accumulates in the bone and can serve as

a source of chronic low-dose exposure (Guandalini *et al.*, 2011; Kelly *et al.*, 2012). We also observed an accumulation of tungsten in the bone. Surprisingly, when compared with tungsten-exposed, non-tumor-bearing BALB/c mice, the tumor-bearing mice had 2-fold more tungsten in the bone. This suggests that the presence of tumor influenced tungsten deposition in the bone. Two of the breast cancer patients, who chose to have mastectomies to remove all residual tungsten from the breast, had detectable tungsten in the urine over 2 years later, suggesting that a secondary reservoir likely exists. Based on our animal data, we hypothesize that this secondary reservoir is the bone. Our work also suggests that these cancer patients may have an

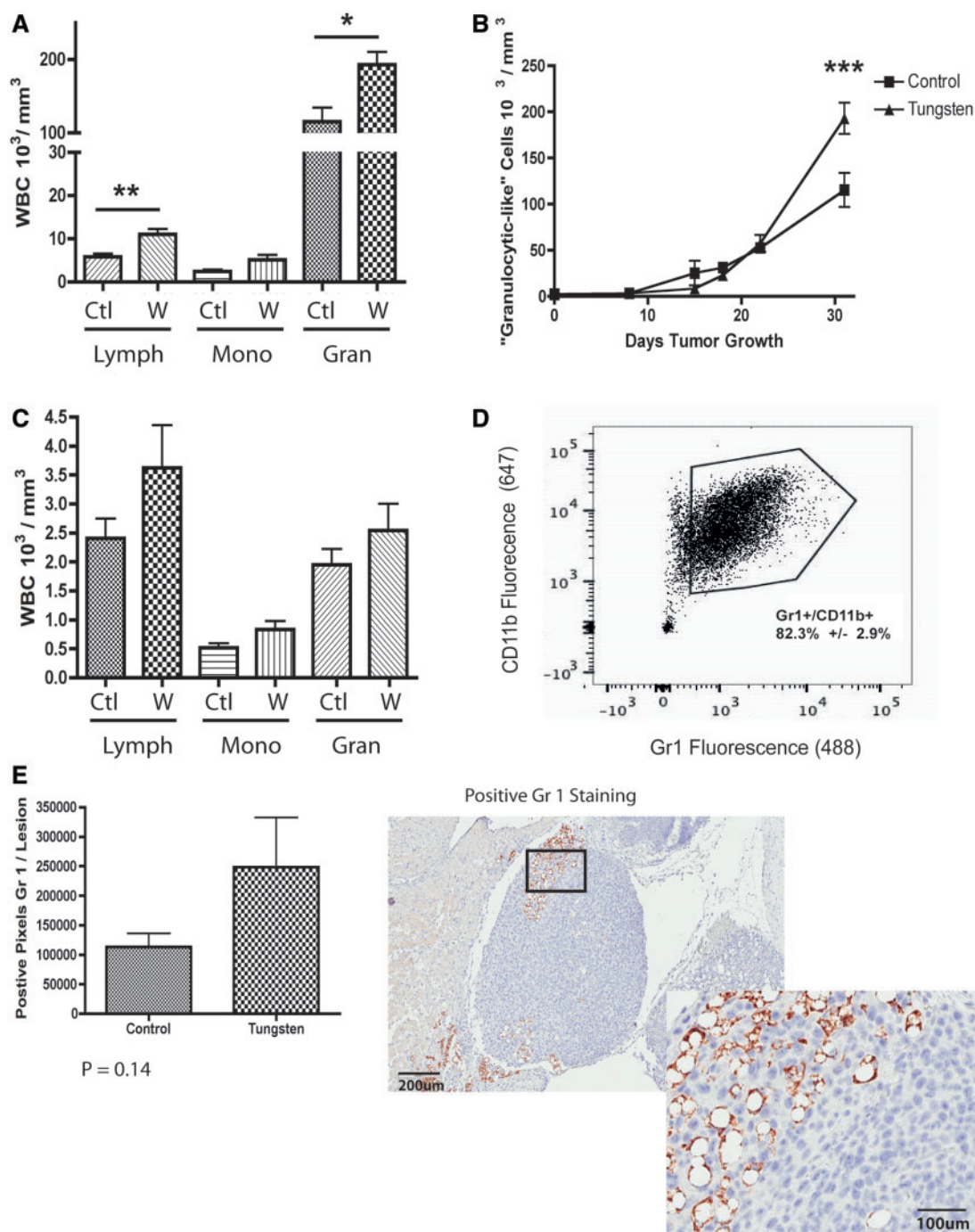


FIG. 7. Tungsten increases the number of myeloid-derived suppressor cells. **A**, White blood cell analysis in peripheral blood at Day 31 of tumor growth in tumor-bearing animals. Graph shows the mean number of white blood cells \pm SE (Lymph = lymphocytes, Mono = monocytes, Gran = granulocytes) for control (C) and tungsten-exposed (W) animals (C: $n=5$, W: $n=7$). * $P < 0.05$, ** $P < 0.01$ unpaired Student's t test. **B**, Number of granulocytic-like cells in the peripheral blood throughout tumor progression in tumor-bearing mice. Graph shows mean number of granulocytic-like cells \pm SE for each group (control: $n=6$, tungsten: $n=7$). *** $P < 0.001$, 2-way ANOVA. **C**, White blood cell analysis in the peripheral blood of non-tumor-bearing animals at 8 weeks. Graph same as part A, for non-tumor-bearing animals ($n=10$). **D**, Flow cytometry analysis of peripheral white blood cells, stained with fluorescent-antibodies Gr1 (AF-488) and CD11b (APC 647). Representative dot plot graph. Mean percentage of Gr1⁺/CD11b⁺ cells in the peripheral blood \pm SE calculated from 7 tumor-bearing mice. **E**, Number of positive Gr1 pixels within and surrounding metastatic lesions in the lung. Graph shows the mean \pm SE in tumor-bearing animals. Unpaired Student's t test. Representative images showing Gr1 positive staining in metastatic lesions (10 \times and 20 \times).

altered tungsten deposition in the bone compared with healthy individuals, but further investigations will be required to make these conclusions.

Perhaps, the presence of the primary tumor is altering bone integrity, which subsequently influences tungsten deposition.

Altered bone remodeling is a common characteristic of various types of cancer that metastasize to the bone, including breast. During bone metastasis, destruction of bone results from increased differentiation and activity of bone marrow-resident osteoclasts in response to tumor cells (Grano *et al.*, 2000). During

normal bone remodeling, macrophages and monocytes are the primary osteoclast precursors (Udagawa *et al.*, 1990), but during breast cancer metastasis to the bone, MDSCs can serve as osteoclast precursors, leading to increased bone destruction (Sawant *et al.*, 2013). Given the data presented here, we hypothesize that bone metastasis will also be altered by tungsten.

Tungsten deposition may also result in the release of other minerals from the bone matrix such as molybdenum, magnesium, calcium, or phosphate, which in turn could be the causative agent leading to the enhanced lung metastasis observed. Interestingly, lead toxicity results in a significant increase in serum calcium, phosphorus, copper, and iron levels (Taha *et al.*, 2013). Although there was no direct indication that these minerals were released from the bone, it does provide evidence that metal accumulation can result in changes in systemic mineral concentrations. Based on their structural similarity, it has been proposed that tungsten can replace phosphate in the bone (Fleshman *et al.*, 1966) and can replace molybdenum in molybdenum-dependent enzymes (Johnson *et al.*, 1974). It is feasible that tungsten deposition could replace other essential minerals present in the bone matrix. A detailed analysis of bone mineral composition in response to tungsten exposure would provide insight into the potential effects of tungsten on bone mineral composition and how those changes could affect tungsten-enhanced metastasis in this model.

Metastasis is a complex multistep process that requires the dissemination of a subset of primary tumor cells into the circulation to a distant secondary site where they colonize and grow. Both intrinsic cellular changes in the primary tumor cells, as well as cellular and extracellular regulators in the tumor microenvironment, are required to initiate and promote this invasive process. We identified that two important cellular regulators of metastasis, CAFs and MDSCs were increased under tungsten exposure in this model. Importantly, MDSCs and CAFs do not work independently, but actually work in concert to promote metastasis. MDSCs and CAFs produce MMPs in order to promote tumor cell invasion and metastasis (Olaso *et al.*, 1997; Stuelten *et al.*, 2005; Yan *et al.*, 2010). These MMPs can, in turn, promote further MDSC mobilization from the bone marrow (Heissig *et al.*, 2002). In addition, increased levels of Pro-MMP-9 in the circulation have been shown to mobilize VEGF, which can act as a ligand to bind to the VEGF receptor on MDSCs and induces clonal expansion (Melani *et al.*, 2007). MMPs, MDSCs, and CAFs all can enhance angiogenesis (Brown *et al.*, 1999; Yang *et al.*, 2004), but we did not observe statistical differences in staining of the angiogenic marker CD31 between control and tungsten-exposed metastatic lesions (data not shown). Thus, future work will focus on investigating how tungsten alters this dynamic network of factors present in the tumor microenvironment in order to promote metastasis. Interestingly, expression of matrix-remodeling and activated fibroblast gene expression signatures in the tumor microenvironment is associated with a poor prognostic outcome in breast cancer patients (Finak *et al.*, 2008), which further highlights the importance of evaluating the tumor microenvironment composition to better understand tumor progression and metastasis.

Our data indicate that tungsten acts as a promoter of metastases, and that those individuals exposed to high levels of tungsten should be frequently monitored for changes in health status. Currently, tungsten concentrations are not routinely monitored in the environment in the United States or Canada. Yet, there are select examples of high-level exposures occurring in both occupational and environmental settings. In a hard metals plant, the concentration of tungsten particulate in the

atmosphere ranged from 0.75 to 6.1 mg/m³, resulting in blood concentrations of tungsten that ranged from 0.8 to 1.1 ppm and urinary concentrations that ranged from 0.6 to 1.1 ppm (NIOSH, 1977). Notably, these tungsten concentrations are substantially higher than those observed in the breast cancer patients. High levels of tungsten from air and ground water sources occur especially near tungsten mines and manufacturing sites. High tungsten levels in drinking water were found near 3 pediatric leukemia clusters in the United States, that are also near tungsten mines (Rubin *et al.*, 2007). In one of these towns, Fallon, Nevada, the highest level of tungsten measured was 742 ppb in the ground water (Seiler, 2005). In children evaluated from this region, the mean urinary tungsten concentration was 2.31 ppb, which was significantly higher than national urinary tungsten concentrations observed in the National Health and Nutritional Examination Survey (0.08 ppb tungsten; CDC, 2003).

Our study shows, for the first time, that tungsten exposure is linked to enhanced metastasis in an animal model, supporting the idea that tungsten can act as a tumor promoter. However, this study does have some limitations. In this study, we focused on one orthotopic breast cancer model, using a fairly aggressive tumor cell line. Investigation of other breast cancer models that preferentially metastasize to other organs or have a weaker metastatic potential, or even other primary tumor types will be informative. Given that tungsten targets the tumor microenvironment instead of the primary tumor to promote metastasis, it is possible that this effect could extend to other cancer models. In addition, investigating the protumor effects over a range of tungsten concentrations would define levels of tungsten exposure where more intensive monitoring should be instituted. Finally, based on this study, it is difficult to determine the potential effect of tungsten on metastasis in humans. An evaluation of cancer and metastasis incidence rates in human populations exposed to high levels of tungsten, especially in areas where tungsten coexists with other potential carcinogens in the environment, could provide evidence regarding the potential of tungsten exposure to promote tumor metastasis in human populations.

ACKNOWLEDGMENT

Authors have no competing financial interests to declare.

FUNDING

The Canadian Institutes of Health Research (MOP-115000 to K.K.M. and MOP-111143 to J.U.-S.); A.M.B. is a postdoctoral fellow with the Cole Foundation.

REFERENCES

- Anard, D., Kirsch-Volders, M., Elhajouji, A., Belpaeme, K., and Lison, D. (1997). In vitro genotoxic effects of hard metal particles assessed by alkaline single cell gel and elution assays. *Carcinogenesis* **18**, 177–184.
- Aslakson, C. J., and Miller, F. R. (1992). Selective events in the metastatic process defined by analysis of the sequential dissemination of subpopulations of a mouse mammary tumor. *Cancer Res.* **52**, 1399–1405.
- Beyersmann, D., and Hartwig, A. (2008). Carcinogenic metal compounds: recent insight into molecular and cellular mechanisms. *Arch. Toxicol.* **82**, 493–512.
- Brown, L. F., Guidi, A. J., Schnitt, S. J., Van De Water, L., Iruela-Arispe, M. L., Yeo, T. K., Tognazzi, K., and Dvorak, H. F. (1999).

- Vascular stroma formation in carcinoma in situ, invasive carcinoma, and metastatic carcinoma of the breast. *Clin. Cancer Res.* **5**, 1041–1056.
- CDC. (2003). Second national report on human exposure to environmental chemicals. Available at: http://www.jhsph.edu/research/centers-and-institutes/center-for-excellence-in-environmental-health-tracking/Second_Report.pdf. Accessed March 15, 2014.
- Chambers, A. F., Groom, A. C., and MacDonald, I. C. (2002). Dissemination and growth of cancer cells in metastatic sites. *Nat. Rev. Cancer* **2**, 563–572.
- Dexter, D. L., Kowalski, H. M., Blazar, B. A., Fligiel, Z., Vogel, R., and Heppner, G. H. (1978). Heterogeneity of tumor cells from a single mouse mammary tumor. *Cancer Res.* **38**, 3174–3181.
- EPA. (2008). Emerging contaminant tungsten. Fact sheet. 505-F-070-005.
- Fastje, C. D., Harper, K., Terry, C., Sheppard, P. R., and Witten, M. L. (2012). Exposure to sodium tungstate and respiratory syncytial virus results in hematological/immunological disease in C57BL/6j mice. *Chem. Biol. Interact.* **196**, 89–95.
- Finak, G., Bertos, N., Pepin, F., Sadekova, S., Souleimanova, M., Zhao, H., Chen, H., Omeroglu, G., Meterissian, S., Omeroglu, A., et al. (2008). Stromal gene expression predicts clinical outcome in breast cancer. *Nat. Med.* **14**, 518–527.
- Fleshman, D., Krokz, S., and Silva, A. (1966). The metabolism of elements of high atomic number. *Univ. Calif. Radiat. Lab.* **14739**, 69–86.
- Grano, M., Mori, G., Minielli, V., Cantatore, F. P., Colucci, S., and Zallone, A. Z. (2000). Breast cancer cell line MDA-231 stimulates osteoclastogenesis and bone resorption in human osteoclasts. *Biochem. Biophys. Comm.* **270**, 1097–1100.
- Guandalini, G. S., Zhang, L., Fornero, E., Centeno, J. A., Mokashi, V. P., Ortiz, P. A., Stockelman, M. D., Osterburg, A. R., and Chapman, G. G. (2011). Tissue distribution of tungsten in mice following oral exposure to sodium tungstate. *Chem. Res. Toxicol.* **24**, 488–493.
- Health Canada. (2013). Second report on human biomonitoring of environmental chemicals in Canada. Available at: www.healthcanada.gc.ca/biomonitoring. Accessed February 26, 2014.
- Heissig, B., Hattori, K., Dias, S., Friedrich, M., Ferris, B., Hackett, N. R., Crystal, R. G., Besmer, P., Lyden, D., Moore, M. A., et al. (2002). Recruitment of stem and progenitor cells from the bone marrow niche requires MMP-9 mediated release of kit ligand. *Cell* **109**, 625–637.
- Johnson, J. L., Rajagopalan, K. V., and Cohen, H. J. (1974). Molecular basis of the biological function of molybdenum. Effect of tungsten on xanthine oxidase and sulfite oxidase in the rat. *J. Biol. Chem.* **249**, 859–866.
- Kalinich, J. F., Emond, C. A., Dalton, T. K., Mog, S. R., Coleman, G. D., Kordell, J. E., Miller, A. C., and McClain, D. E. (2005). Embedded weapons-grade tungsten alloy shrapnel rapidly induces metastatic high-grade rhabdomyosarcomas in F344 rats. *Environ. Health Perspect.* **113**, 729–734.
- Kaplan, R. N., Riba, R. D., Zacharoulis, S., Bramley, A. H., Vincent, L., Costa, C., MacDonald, D. D., Jin, D. K., Shido, K., Kerns, S. A., et al. (2005). VEGFR1-positive haematopoietic bone marrow progenitors initiate the pre-metastatic niche. *Nature* **438**, 820–827.
- Keith, L. S., Wohlers, D. W., Moffett, D. B., Rosemond, Z. A.; Agency for Toxic Substances and Disease Registry. (2007). ATSDR evaluation of potential for human exposure to tungsten. *Toxicol. Ind. Health* **23**, 309–345.
- Kelly, A. D., Lemaire, M., Young, Y. K., Eustache, J. H., Guilbert, C., Flores Molina, M., and Mann, K. K. (2012). In vivo tungsten exposure alters B cell development and increases DNA damage in murine bone marrow. *Toxicol. Sci.* **131**, 434–446.
- Kusmartsev, S., Nefedova, Y., Yoder, D., and Gabrilovich, D. I. (2004). Antigen-specific inhibition of CD8+ T cell response by immature myeloid cells in cancer is mediated by reactive oxygen species. *J. Immunol.* **172**, 989–999.
- Melani, C., Sangaletti, S., Barazzetta, F. M., Werb, Z., and Colombo, M. P. (2007). Amino-biphosphonate-mediated MMP-9 inhibition breaks the tumor-bone marrow axis responsible for myeloid-derived suppressor cell expansion and macrophage infiltration in tumor stroma. *Cancer Res.* **67**, 11438–11446.
- Miller, A. C., Mog, S., McKinney, L., Luo, L., Allen, J., Xu, J., and Page, N. (2001). Neoplastic transformation of human osteoblast cells to the tumorigenic phenotype by heavy metal-tungsten alloy particles: induction of genotoxic effects. *Carcinogenesis* **22**, 115–125.
- NIOSH. (1977). Criteria for a Recommended Standard: Occupational exposure to tungsten and cemented carbide. Publication Number 77-227.
- Nozaki, S., Sissons, S., Chien, D. S., and Sledge, G. W., Jr. (2003). Activity of biphenyl matrix metalloproteinase inhibitor BAY 12-9566 in a human breast cancer orthotopic model. *Clin. Exp. Metastasis* **20**, 407–412.
- Olaso, E., Santisteban, A., Bidaurrazaga, J., Gressner, A. M., Rosenbaum, J., and Vidal-Vanaclocha, F. (1997). Tumor-dependent activation of rodent hepatic stellate cells during experimental melanoma metastasis. *Hepatology* **26**, 634–642.
- Paschal, D. C., Ting, B. G., Morrow, J. C., Pirkle, J. L., Jackson, R. J., Sampson, E. J., Miller, D. T., and Caldwell, K. L. (1998). Trace metals in urine of United States residents: reference range concentrations. *Environ. Res.* **76**, 53–59.
- Planas-Bohne, F. (1979). Influence of several chelating agents on the excretion and organ concentration of copper in the rat. *Toxicol. Appl. Pharm.* **50**, 337–345.
- Rubin, C. S., Holmes, A. K., Belson, M. G., Jones, R. L., Flanders, W. D., Kieszak, S. M., Osterloh, J., Luber, G. E., Blount, B. C., Barr, D. B., et al. (2007). Investigating childhood leukemia in Churchill County, Nevada. *Environ. Health Perspect.* **115**, 151–157.
- Sawant, A., Deshane, J., Jules, J., Lee, C. M., Harris, B. A., Feng, X., and Ponnazhagan, S. (2013). Myeloid-derived suppressor cells function as novel osteoclast progenitors enhancing bone loss in breast cancer. *Cancer Res.* **73**, 672–682.
- Seiler, R. L., Stollenwerk, K.G. and Garbarino, J. K. (2005). Factors controlling tungsten concentrations in ground water, Carson Desert, Nevada. *Appl. Geochem.* **20**, 423–441.
- Stuelten, C. H., DaCosta Byfield, S., Arany, P. R., Karpova, T. S., Stetler-Stevenson, W. G., and Roberts, A. B. (2005). Breast cancer cells induce stromal fibroblasts to express MMP-9 via secretion of TNF-alpha and TGF-beta. *J. Cell Sci.* **118**(Pt 10), 2143–2153.
- Taha, N. M., Korshom, M. S., Mandoura, E. M., Lebda, M. A., Aladham, E. S. (2013). Effect of lead toxicity on mineral metabolism and immunological factors in rats. *AJVS* **39**, 64–73.
- Tyrrell, J., Galloway, T. S., Abo-Zaid, G., Melzer, D., Depledge, M. H., and Osborne, N. J. (2013). High urinary tungsten concentration is associated with stroke in the National Health and Nutrition Examination Survey 1999–2010. *PLoS One* **8**, 1–7.
- Udagawa, N., Takahashi, N., Akatsu, T., Tanaka, H., Sasaki, T., Nishihara, T., Koga, T., Martin, T. J., and Suda, T. (1990).

- Origin of osteoclasts: mature monocytes and macrophages are capable of differentiating into osteoclasts under a suitable microenvironment prepared by bone marrow-derived stromal cells. *Proc. Natl Acad. Sci.* **87**, 7260–7264.
- Wei, H. J., Luo, X. M., and Yang, S. P. (1985). Effects of molybdenum and tungsten on mammary carcinogenesis in SD rats. *J. Natl Cancer Inst.* **74**, 469–473.
- Xu, Z. F., and Jones, M. M. (1988). Comparative mobilization of lead by chelating agents. *Toxicology* **53**, 277–288.
- Yan, H. H., Pickup, M., Pang, Y., Gorska, A. E., Li, Z., Chytil, A., Geng, Y., Gray, J. W., Moses, H. L., and Yang, L. (2010). Gr-1+CD11b+ myeloid cells tip the balance of immune protection to tumor promotion in the premetastatic lung. *Cancer Res.* **70**, 6139–6149.
- Yang, L., DeBusk, L. M., Fukuda, K., Fingleton, B., Green-Jarvis, B., Shyr, Y., Matrisian, L. M., Carbone, D. P., and Lin, P. C. (2004). Expansion of myeloid immune suppressor Gr+CD11b+ cells in tumor-bearing host directly promotes tumor angiogenesis. *Cancer Cell* **6**, 409–421.
- Yu, Y., Xiao, C. H., Tan, L. D., Wang, Q. S., Li, X. Q., and Feng, Y. M. (2014). Cancer-associated fibroblasts induce epithelial-mesenchymal transition of breast cancer cells through paracrine TGF-beta signalling. *Br. J. Cancer* **110**, 724–732.